SUPPLEMENTAL INFORMATION

Environmental Enrichment Rescues Binocular Matching of Orientation Preference in Mice with a Precocious Critical Period

Bor-Shuen Wang[1,3], Liang Feng[2], Mingna Liu[1], Xiaorong Liu[1,2,*], and Jianhua Cang[1,*]

1. Department of Neurobiology,

2. Department of Ophthalmology,

3. Interdepartmental Neuroscience Program,

Northwestern University, Evanston, Illinois 60208

*Correspondence:

Jianhua Cang, cang@northwestern.edu, 1-847-467-0478; and

Xiaorong Liu, xiaorong-liu@northwestern.edu, 1-847-467-0529.

Including 5 figures, 1 table, 1 video and supplemental experimental procedure.

SUPPLEMENTAL FIGURES

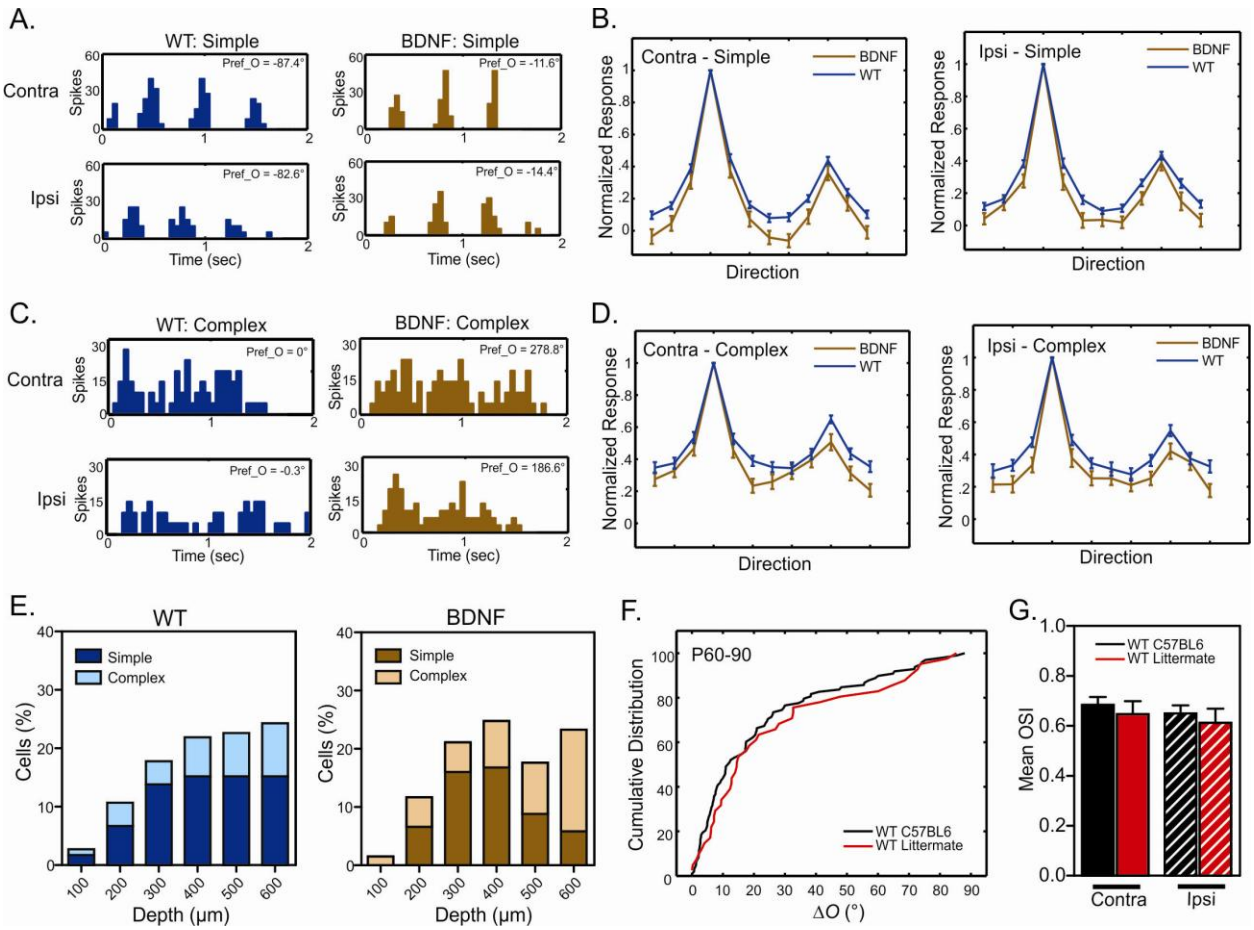

Figure S1. Binocular matching in BDNF-OE mice. Related to Figure 1.

(A-D) Peri-stimulus timing histograms (PSTHs) of example cells at their preferred directions (A and C) and mean tuning curves (B and D) through the 2 eyes are shown separately for simple and complex cells for WT (blue) and BDNF-OE (brown) mice. The "Pref_O" values in individual panels of A and C are the cell's preferred orientation through that eye. Note that only the complex cell in the BDNF-OE mouse was mismatched. (E) Distribution of the recorded simple and complex cells at different cortical depths in the two genotypes. (F-G) Similar binocular matching and orientation selectivity between WT C57Bl6 mice and the WT littermate controls of the BDNF-OE mice. Cumulative distribution of ΔO in the two WT groups are shown in panel F ($P = 0.52$) and OSI between the two groups in panel G (Contra: $P = 0.60$; Ipsi: $P = 0.52$).

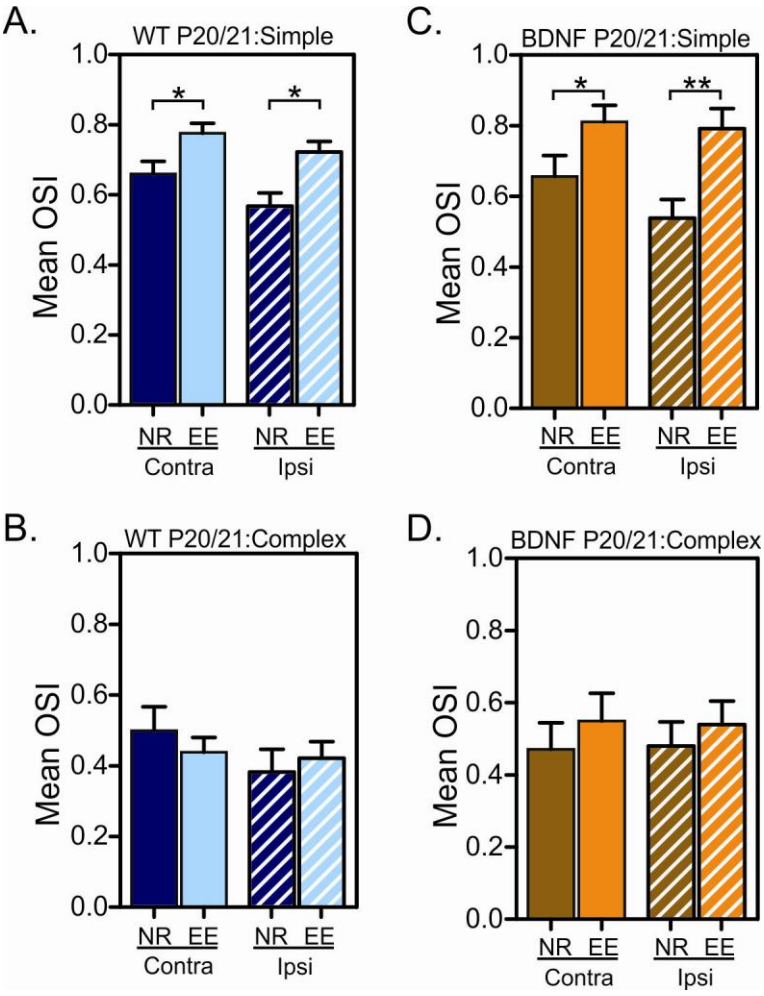

Figure S2. Environmental enrichment accelerates the development of simple cell orientation selectivity in WT and BDNF-OE mice. Related to Figure 4.

(A-B) Mean OSI of simple (A) and complex (B) cells in WT mice reared in normal (NR) and enriched environment (EE). Monocular orientation tuning improves significantly with EE and reaches adult level by P20/21 in simple cells, but not complex cells. (C-D) EE improves monocular orientation tuning of simple cells in BDNF-OE mice by P20/21 (C), but not complex cells (D), just as in WT mice.

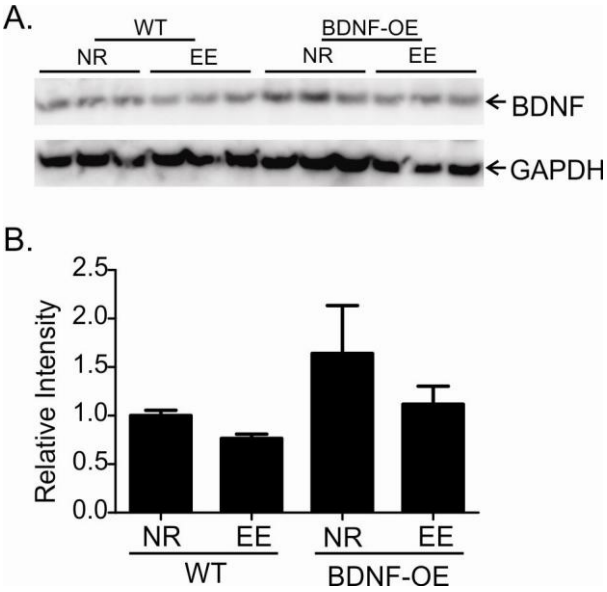

Figure S3. Environmental enrichment does not increase BDNF level at P17. Related to Figure 4. (A) Representative Western blots for BDNF and the sample loading control GAPDH. All samples were collected from the visual cortex of P17 mice. (B) Quantification of relative level of BDNF in WT and BDNF-OE mice, under normal (NR) or enriched (EE) conditions (n = 4 samples in each group, repeated twice). Note that EE did not increase BDNF level at P17, consistent with what was previously shown at a similar age (Cancedda et al., 2004). A trend of decrease was actually seen (P = 0.15, ANOVA).

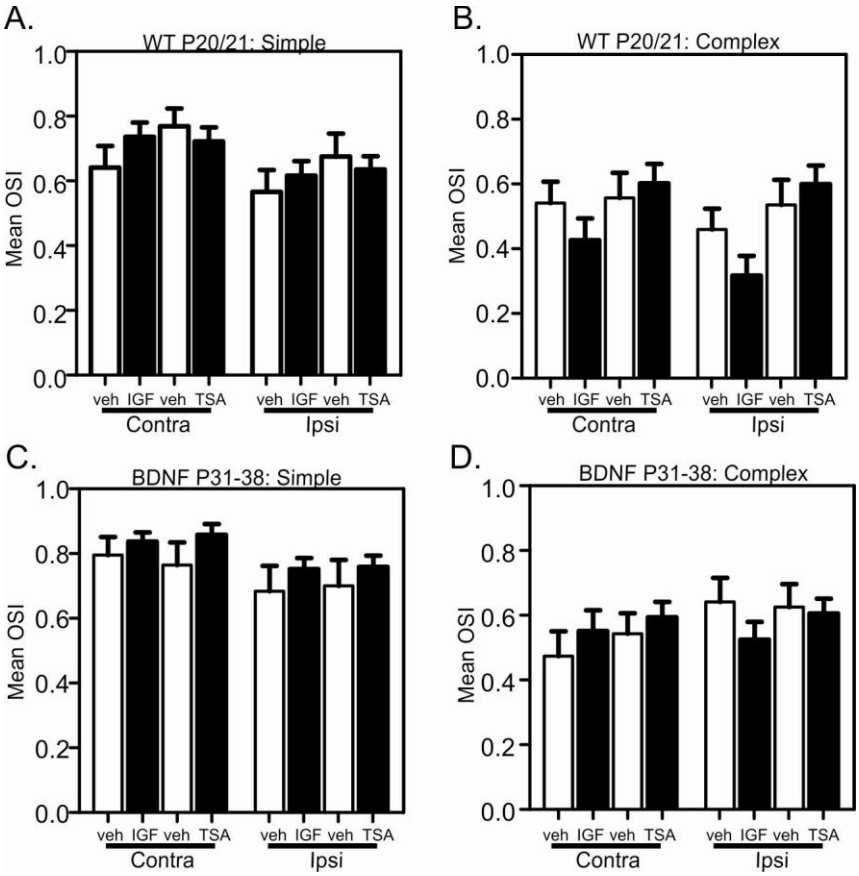

Figure S4. Normal orientation selectivity in IGF-1 and TSA treated mice. Related to Figures 5 and 6.

(A-B) Mean OSI in IGF-1 or TSA treated P20/21 WT mice and their respective vehicle-treated controls. (C-D) Mean OSI in IGF-1 or TSA treated P31-38 BDNF-OE mice and their respective vehicle-treated controls. No significant difference was seen in comparing any groups with their controls.

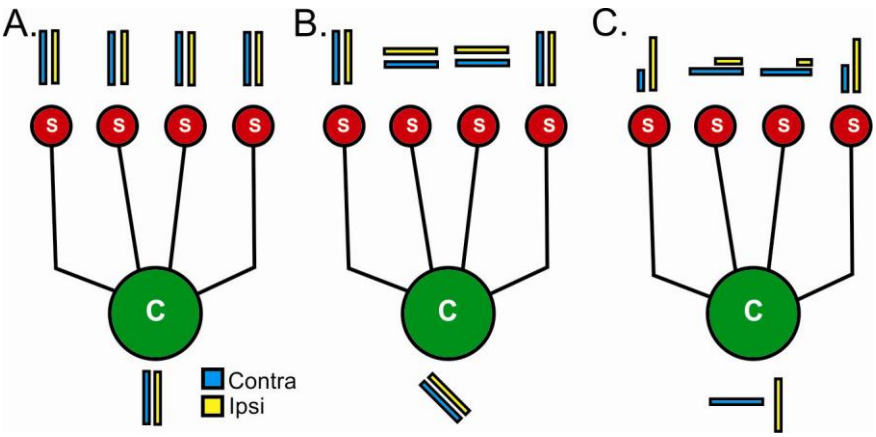

Figure S5. Schematics of binocular matching of simple and complex cells. Related to Figure 2. (A) If the presynaptic simple cells ("s") are all tuned to the same orientation, the complex cell ("C") would be automatically matched binocularly after the matching of simple cells. The orientation tuning of each cell is represented by the orientation of the short bars, with blue through the contralateral eye and yellow from the ipsilateral eye. (B) If the simple cells are individually tuned to a wide range of orientations, the orientation preference of the complex cell through either eye is determined by the summation of the heterogeneously-tuned synaptic inputs. Complex cells would still be automatically matched after simple cells matching, if the input cells all have similar ocular dominance levels (as represented by the length of the two bars). (C) Pooling the inputs of simple cells that have diverse ocular dominance and heterogeneous orientation preference would result in a binocular mismatch in the complex cell, even if the simple cells are binocularly matched.

Table S1: Mean orientation difference (*ΔO*) and orientation selectivity index (OSI) for all experimental groups. Related to all figures.

	Experimental Groups	Mean ΔO						Mean OSI								
								Simple			Complex			All		
		Simple	N	Complex	N	All	N	Contra	Ipsi	N	Contra	Ipsi	N	Contra	Ipsi	N
WT	**P15-18**	31.0 ± 3.8	35	38.6 ± 5.6	25	34.2 ± 3.3	60	0.65 ± 0.06	0.63 ± 0.05	35	0.42 ± 0.06	0.41 ± 0.06	25	0.55 ± 0.04	0.54 ± 0.04	60
	P20/21	33.0 ± 3.1	69	39.2 ± 5.3	28	34.8 ± 2.7	97	0.66 ± 0.04	0.57 ± 0.04	69	0.50 ± 0.07	0.38 ± 0.06	28	0.61 ± 0.03	0.51 ± 0.03	97
	P22/23	18.3 ± 2.7	52	37.6 ± 4.1	38	26.4 ± 2.5	90	0.75 ± 0.04	0.64 ± 0.05	52	0.44 ± 0.05	0.43 ± 0.05	38	0.62 ± 0.04	0.55 ± 0.04	90
	P26/27	20.5 ± 2.5	51	38.5 ± 4.2	39	28.3 ± 2.5	90	0.74 ± 0.04	0.74 ± 0.04	51	0.52 ± 0.05	0.49 ± 0.06	39	0.65 ± 0.03	0.63 ± 0.04	90
	P31-36	19.7 ± 1.9	115	24.4 ± 2.3	84	21.7 ± 1.5	199	0.82 ± 0.02	0.75 ± 0.02	115	0.45 ± 0.04	0.48 ± 0.04	84	0.66 ± 0.02	0.64 ± 0.02	199
	P60-90	18.0 ± 2.5	55	27.2 ± 4.2	43	22.1 ± 2.4	98	0.75 ± 0.04	0.72 ± 0.04	55	0.60 ± 0.05	0.56 ± 0.05	43	0.68 ± 0.03	0.65 ± 0.03	98
	P31-90	19.1 ± 1.5	170	25.4 ± 2.0	127	21.8 ± 1.2	297	0.79 ± 0.02	0.74 ± 0.02	170	0.50 ± 0.03	0.51 ± 0.03	127	0.67 ± 0.02	0.64 ± 0.02	297
	DD P31-36	37.7 ± 2.3	135	41.2 ± 2.8	99	39.2 ± 1.8	234	0.76 ± 0.02	0.72 ± 0.02	135	0.47 ± 0.03	0.46 ± 0.03	99	0.64 ± 0.02	0.61 ± 0.02	234
	DZ P31-36	19.8 ± 3.6	39	40.9 ± 4.1	48	31.4 ± 3.0	87	0.74 ± 0.05	0.68 ± 0.05	39	0.51 ± 0.05	0.52 ± 0.05	48	0.61 ± 0.04	0.59 ± 0.03	87
	DZ-Veh P31-36	15.5 ± 4.2	24	21.1 ± 6.1	18	17.9 ± 3.5	42	0.78 ± 0.06	0.79 ± 0.05	24	0.67 ± 0.09	0.57 ± 0.09	18	0.73 ± 0.05	0.70 ± 0.05	42
	IGF-1 P20/21	22.5 ± 3.5	45	31.3 ± 5.2	21	25.3 ± 2.9	66	0.74 ± 0.04	0.62 ± 0.05	45	0.43 ± 0.07	0.32 ± 0.06	21	0.64 ± 0.04	0.52 ± 0.04	66
	IGF-1-Veh P20/21	31.1 ± 5.4	21	35.7 ± 4.2	22	33.4 ± 3.4	43	0.64 ± 0.07	0.57 ± 0.07	21	0.54 ± 0.07	0.46 ± 0.06	22	0.59 ± 0.05	0.51 ± 0.05	43
	TSA P20/21	21.8 ± 2.9	45	22.9 ± 4.0	34	22.3 ± 2.4	79	0.72 ± 0.04	0.64 ± 0.04	45	0.60 ± 0.06	0.60 ± 0.06	34	0.67 ± 0.04	0.62 ± 0.03	79
	TSA-Veh P20/21	36.6 ± 6.3	20	45.6 ± 5.7	21	41.2 ± 4.3	41	0.77 ± 0.05	0.68 ± 0.07	20	0.56 ± 0.08	0.54 ± 0.08	21	0.66 ± 0.05	0.60 ± 0.05	41
BDNF-OE	**P15-18**	36.5 ± 8.5	13	32.6 ± 3.9	40	33.6 ± 3.6	53	0.69 ± 0.09	0.68 ± 0.09	13	0.46 ± 0.05	0.46 ± 0.05	40	0.52 ± 0.05	0.52 ± 0.05	53
	P20/21	34.1 ± 4.5	29	42.7 ± 4.9	22	37.8 ± 3.3	51	0.66 ± 0.06	0.54 ± 0.05	29	0.47 ± 0.07	0.48 ± 0.07	22	0.58 ± 0.05	0.51 ± 0.04	51
	P31-36	23.6 ± 5.2	17	32.5 ± 4.2	27	29.1 ± 3.3	44	0.90 ± 0.04	0.75 ± 0.07	17	0.64 ± 0.06	0.59 ± 0.07	27	0.74 ± 0.04	0.65 ± 0.05	44
	P60-90	24.4 ± 4.1	34	37.1 ± 3.7	59	33.4 ± 2.9	93	0.82 ± 0.05	0.78 ± 0.04	34	0.59 ± 0.05	0.56 ± 0.04	59	0.68 ± 0.04	0.64 ± 0.03	93
	P31-90	24.2 ± 3.2	51	35.7 ± 2.9	86	32.0 ± 2.2	137	0.85 ± 0.04	0.77 ± 0.04	51	0.61 ± 0.04	0.56 ± 0.04	86	0.70 ± 0.03	0.64 ± 0.03	137
	IGF-1 P31-38	21.9 ± 2.6	74	24.7 ± 3.8	38	22.9 ± 2.2	112	0.84 ± 0.03	0.75 ± 0.03	74	0.55 ± 0.06	0.53 ± 0.05	38	0.74 ± 0.03	0.68 ± 0.03	112
	IGF-1-Veh P31-38	26.0 ± 5.4	15	39.4 ± 4.9	24	34.2 ± 3.8	39	0.80 ± 0.06	0.68 ± 0.08	15	0.47 ± 0.08	0.64 ± 0.07	24	0.60 ± 0.06	0.66 ± 0.05	39
	TSA P31-38	20.4 ± 2.7	60	28.0 ± 3.5	61	24.2 ± 2.2	121	0.86 ± 0.03	0.76 ± 0.04	60	0.59 ± 0.05	0.61 ± 0.05	61	0.73 ± 0.03	0.68 ± 0.03	121
	TSA-Veh P31-38	25.1 ± 6.6	14	49.9 ± 4.0	27	41.4 ± 3.9	41	0.76 ± 0.07	0.70 ± 0.08	14	0.54 ± 0.06	0.63 ± 0.07	27	0.62 ± 0.05	0.65 ± 0.05	41
WT-EE	**P15-18**	37.5 ± 3.5	57	40.5 ± 3.6	53	38.9 ± 2.5	110	0.65 ± 0.04	0.53 ± 0.04	57	0.42 ± 0.05	0.48 ± 0.05	53	0.54 ± 0.03	0.51 ± 0.03	110
	P20/21	20.6 ± 2.3	78	26.5 ± 3.2	51	22.9 ± 1.9	129	0.78 ± 0.03	0.72 ± 0.03	78	0.44 ± 0.04	0.42 ± 0.05	51	0.64 ± 0.03	0.60 ± 0.03	129
BDNF-EE	**P15-18**	36.0 ± 4.3	46	34.7 ± 4.5	29	35.5 ± 3.2	75	0.62 ± 0.04	0.59 ± 0.04	46	0.42 ± 0.06	0.38 ± 0.06	29	0.54 ± 0.04	0.51 ± 0.04	75
	P20/21	18.2 ± 3.6	29	24.2 ± 5.5	23	20.8 ± 3.2	52	0.81 ± 0.05	0.79 ± 0.06	29	0.55 ± 0.08	0.54 ± 0.06	23	0.69 ± 0.05	0.68 ± 0.05	52
	P31-36	23.2 ± 3.4	48	21.8 ± 3.5	41	22.6 ± 2.4	89	0.83 ± 0.04	0.77 ± 0.04	48	0.66 ± 0.05	0.64 ± 0.06	41	0.75 ± 0.03	0.71 ± 0.03	89
	EE-NR P31-36	17.7 ± 2.6	58	23.8 ± 2.9	63	20.9 ± 2.0	121	0.83 ± 0.03	0.80 ± 0.03	58	0.60 ± 0.05	0.64 ± 0.04	63	0.71 ± 0.03	0.72 ± 0.03	121

Movie S1. A movie of the environmental enrichment condition. Related to Figure 4.

SUPPLEMENTAL EXPERIMENTAL PROCEDURES

Mice and Rearing conditions

Wildtype C57BL/6 mice and BDNF-OE mice (Huang et al., 1999) of different ages and both genders were used in this study. The BDNF-OE mice were purchased from the Jackson Laboratory (stock # 006579) and maintained locally by crossing BDNF-OE males with WT C57BL/6 females. The resulting offspring were screened for the transgene by PCR (Huang et al., 1999). The orientation tuning and binocular matching of the transgene negative littermates were confirmed to be comparable to WT C57BL/6 mice (Figure S1). We thus combined the two groups together as WT controls. All animals were used in accordance with protocols approved by Northwestern University Institutional Animal Care and Use Committee.

Mice were reared either under standard condition or in enriched environment (EE). In the standard condition, pups were housed with their dams in standard mouse cages (12 × 7 × 5 in). They were either recorded at P15-18 (n = 18 for WT, and n = 14 for BDNF-OE), P20/21 (n = 17 for WT, and n = 7 for BDNF-OE), or weaned at P21. The weanlings were then housed in the same size cages with maximum occupancy of five, until the day of recording (P22/23: n = 12 for WT; P26/27: n = 8 for WT; P31-36: n = 18 for WT, n = 4 for BDNF-OE; P60-90: n = 15 for WT, n = 8 for BDNF-OE). Note that some of the WT data were already included in our previous publication (Wang et al., 2010a). The enriched environment consisted of a larger cage (18 × 14 × 8 in) that contained a number of toys, including crawl balls, pup tents, huts, tunnels, balls, and a running wheel. The toys were repositioned once every two days and replaced with new ones once per week (Cancedda et al., 2004). Visual posters were placed around the cages and were repositioned every two days. Every enriched cage housed at least two experienced dams and 3-4 additional filler females. The dams were impregnated in standard cages and transferred to the

enriched cages 4-5 days before delivery. The pups were then born and reared in the enriched cage (EE) until the day of recording (P15-P18: n = 19 for WT and n = 12 for BDNF-OE; P20/21: n = 16 for WT and n = 4 for BDNF-OE; P31-36: n = 11 for BDNF-OE). For short term enrichment experiments (EE-NR), the pups were born and raised in the enriched cage until P17, then the pups and the mom were relocated into the standard cages until the day of recording P31-P36 (n = 10). All animals in both rearing conditions were housed in 12h light:12h dark cycle.

To determine the degree of binocular matching in the absence of any visual experience, WT mice (n = 63) in standard rearing conditions were placed in complete darkness starting from P11, before eye-opening until the day of the experiment (P31-36). The dark-reared dataset included mice (n = 57) for another study (Sarnaik et al., 2013).

Antibodies used in western blot analysis

Antibodies included: Acetyl-Histone H3 (Lys9) Rabbit pAb (Cat#9671, 1:1500, Cell Signaling, MA), Histone H3 (D1H2) Rabbit mAb (Cat#4499, 1:10000, Cell Signaling, MA), Acetyl-Histone H4 (Lys5) Rabbit pAb (Cat#9672, 1:1500, Cell Signaling, MA), Histone H4 Rabbit pAb (Cat#ab10158, 1:2000, Abcam, MA), BDNF (N-20) Rabbit pAb (Cat#sc-546, 1:400; Santa Cruz Biotechnology, Santa Cruz, CA), and Glyceraldehyde-3-Phosphate Dehydrogenase (GAPDH) Mouse mAb (Cat#MAB374, 1:2000, EMD Millipore, MA).

In vivo physiology

Mice of various ages were anesthetized using urethane (1.2-1.3g/kg in 10% saline solution, i.p.) and supplemented by the sedative chlorprothixene (10mg/kg, i.m.) as described previously (Cang et al., 2008; Wang et al., 2010a; Wang et al., 2009; Wang et al., 2010b). Atropine (0.3 mg/kg) and dexamethasone (2.0 mg/kg) were injected subcutaneously. Additional urethane (0.2-0.3g/kg)

was administered as needed. The eyes of the animal were covered by silicone oil to avoid drying. The animal was placed in a stereotaxic apparatus on a heating pad. The animal's temperature was monitored with a rectal thermoprobe and maintained at 37°C through a feedback heater control module (Frederick Haer Company, Bowdoinham, ME). Electrocardiograph leads were attached across the skin to monitor the heart rate continuously throughout the experiment. A tracheotomy was performed only in mice older than P30.

A small craniotomy (~2 mm^2) was performed at the left hemisphere to expose the cortex for recording. 5-10 MΩ tungsten microelectrodes (FHC, Bowdoinham, ME) were penetrated perpendicular to the pial surface in the binocular zone of V1 (2.8-3.3 mm lateral from the midline and 0.5-0.8 mm anterior from the lambda suture). In each animal, 2-6 penetrations were made with minimum spacing of 50 μm and cells recorded across all layers were included in our analysis. Electrical signals, both spikes (filtered between 0.3 and 5 KHz and sampled at 25 KHz) and field potentials (filtered between 10 and 300 Hz and sampled at 800 Hz), were acquired using a System 3 workstation (Tucker Davis Technologies, FL) and the spike waveforms were further sorted offline into single units using OpenSorter (Tucker Davis Technologies, FL). The animals were overdosed with Euthasol (150 mg/kg pentobarbital; Virbac) at the end of recording.

Visual stimuli and analysis followed our previous study (Wang et al., 2010a). Briefly, visual stimuli were generated with Matlab programs (Niell and Stryker, 2008) using the Psychophysics Toolbox extensions (Brainard, 1997; Pelli, 1997). A CRT video monitor (40 × 30 cm, 60 Hz refresh rate, ~35 cd/m^2 mean luminance), was placed at 25 cm in front of the animal to display the stimuli, with its midline aligned with the animal. The stimulus was delivered through either eye separately; i.e. the stimulus was delivered through the eye contralateral to the recorded hemisphere while the ipsilateral eye was occluded, and vice versa.

Optical imaging of ocular dominance plasticity

Monocular deprivation of the right eye was performed in WT, WT-EE and BDNF-OE mice at P15 under isofluorane anesthesia (1.5-2% in O_2) following published procedures (Cang et al., 2005; Sato and Stryker, 2008). Mice whose eyelids were not completely sealed close or those with any indication of corneal damage or cataracts were excluded from the study before imaging. The ocular dominance of these mice was determined 5-6 days later by optical imaging of intrinsic signals (Cang et al., 2005; Kalatsky and Stryker, 2003; Sato and Stryker, 2008). Briefly, the animals were anesthetized and prepared with the same protocol described in the *in vivo* physiology section. A craniotomy was preformed to expose the left visual cortex, and the cortex was then covered with agarose and coverslip to form an imaging window. The visual stimulus was a thin bar (2° in height and 20° in width) drifting continuously and periodically upward or downward. It was shown between -5° to 15° azimuth (the vertical meridian defined as 0° with negative values for ipsilateral visual field) and full-screen elevations. The spatial frequency of the drifting bar was 1 cycle/100°, and temporal frequency 1 cycle/8 s. Optical images were acquired at 610 nm using a Dalsa 1M30 CCD camera (Dalsa, Waterloo, Canada) and the Fourier component of the reflectance changes was extracted at the temporal frequency of the stimulus as described previously (Kalatsky and Stryker, 2003).

The response magnitude map evoked by ipsilateral eye stimulation was first smoothed by a uniform kernel of 5×5 filter and then thresholded at 30% of the peak response amplitude, in order to determine the binocular zone for ocular dominance analysis. The ocular dominance index (ODI) was calculated as the mean of $(C - I)/(C + I)$ of all pixels within the selected region, where C and I represent the response magnitude to the contralateral and ipsilateral eyes, respectively (Cang et al., 2005). The ODI ranges from +1 to -1, where a positive value indicates

a contralateral bias, and negative ODI an ipsilateral bias.

REFERENCES

Brainard, D.H. (1997). The Psychophysics Toolbox. Spat Vis *10*, 433-436.

Cancedda, L., Putignano, E., Sale, A., Viegi, A., Berardi, N., and Maffei, L. (2004). Acceleration of visual system development by environmental enrichment. J Neurosci *24*, 4840-4848.

Cang, J., Kalatsky, V.A., Lowel, S., and Stryker, M.P. (2005). Optical imaging of the intrinsic signal as a measure of cortical plasticity in the mouse. Vis Neurosci *22*, 685-691.

Cang, J., Niell, C.M., Liu, X., Pfeiffenberger, C., Feldheim, D.A., and Stryker, M.P. (2008). Selective disruption of one Cartesian axis of cortical maps and receptive fields by deficiency in ephrin-As and structured activity. Neuron *57*, 511-523.

Huang, Z.J., Kirkwood, A., Pizzorusso, T., Porciatti, V., Morales, B., Bear, M.F., Maffei, L., and Tonegawa, S. (1999). BDNF regulates the maturation of inhibition and the critical period of plasticity in mouse visual cortex. Cell *98*, 739-755.

Kalatsky, V.A., and Stryker, M.P. (2003). New paradigm for optical imaging: temporally encoded maps of intrinsic signal. Neuron *38*, 529-545.

Niell, C.M., and Stryker, M.P. (2008). Highly selective receptive fields in mouse visual cortex. J Neurosci *28*, 7520-7536.

Pelli, D.G. (1997). The VideoToolbox software for visual psychophysics: transforming numbers into movies. Spat Vis *10*, 437-442.

Sarnaik, R., Wang, B.S., and Cang, J. (2013). Experience-Dependent and Independent Binocular Correspondence of Receptive Field Subregions in Mouse Visual Cortex. Cereb Cortex.

Sato, M., and Stryker, M.P. (2008). Distinctive features of adult ocular dominance plasticity. J Neurosci *28*, 10278-10286.

Wang, B.S., Sarnaik, R., and Cang, J. (2010a). Critical period plasticity matches binocular orientation preference in the visual cortex. Neuron *65*, 246-256.

Wang, L., Rangarajan, K.V., Lawhn-Heath, C.A., Sarnaik, R., Wang, B.S., Liu, X., and Cang, J. (2009). Direction-specific disruption of subcortical visual behavior and receptive fields in mice lacking the beta2 subunit of nicotinic acetylcholine receptor. J Neurosci *29*, 12909-12918.

Wang, L., Sarnaik, R., Rangarajan, K., Liu, X., and Cang, J. (2010b). Visual receptive field properties of neurons in the superficial superior colliculus of the mouse. J Neurosci *30*, 16573-16584.